Granular systems on a vibrating wall: The kinetic boundary condition

Rodrigo Soto*
Departamento de Física, FCFM, Universidad de Chile, Casilla 487-3, Santiago, Chile
(Received 2 October 2003; revised manuscript received 18 December 2003; published 16 June 2004)

Dense granular media, fluidized by a vibrating wall, is studied in the high-vibrating frequency limit, where the plate vibration frequency is much greater than the collision frequency, and the plate acceleration is much greater than gravity. Using kinetic theory, it is shown that, regardless of the fluid density, external field, or restitution coefficient between particles, there is an asymptotic scaling for saying that if $A\omega$ is kept constant, then different amplitudes A (with the corresponding frequencies ω) produce the same macroscopic result. Furthermore, it is found that in the limit of high frequencies, the boundary condition associated with the vibrating wall can be replaced by a stationary heat source. The value of the heat flux depends linearly with density even for dense fluids. Numerical comparisons with molecular dynamics simulations confirm these predictions and show that the substitution of the vibrating wall by a thermal one gives poor results, while the substitution by a heat source is very accurate.

DOI: 10.1103/PhysRevE.69.061305 PACS number(s): 45.70.−n, 44.10.+i, 51.20.+d

I. INTRODUCTION

Granular matter is usually kept fluidized by means of vibrating walls. Commonly hydrodynamic or kinetic theory approaches are used to describe the bulk of the granular fluid (see, for example, Ref. [1]). However, a detailed consideration of the boundary condition is difficult because of its explicit time dependence. In the case of high frequency and small amplitude vibrations, successive collisions of the grains with the wall are uncorrelated. For this reason, in this limiting case, the wall has been usually modeled as a stochastic border. It has been argued that the wall can be replaced by a thermal wall at a fixed granular temperature, that scales as $T_{\text{wall}} \sim m(A\omega)^2$, where m is the particle mass, and A and ω are the oscillation amplitude and frequency, respectively [2]. Also, kinetic approaches have been used to characterize the vibrating boundary condition in more detail [3], and instead of using a thermal wall, it has been shown that for some types of vibrating walls (sawtooth or triangular waveform) in the dilute case, it imposes a permanent energy influx [5–9].

In this article, we consider the high frequency case, where kinetic equations must be used to describe the layer near the wall. It is shown that, for any waveform of the oscillating wall, in the limiting case $\omega \to \infty$, $A \to 0$, such that $A\omega$ is kept constant, the wall can be effectively replaced by a static wall that imposes a permanent energy influx. The value of the energy influx is linearly proportional to density even for nonideal situations. It also depends on the waveform of the wall, but it is independent of any external field or if the kinetic equation needed to describe the granular dynamics is the Boltzmann, Enskog, or even Liouville equations.

We give an expression for the energy influx for a general wave form. In the case of the sawtooth wave form, we recover the expression given in Refs. [5] and [6], and for the sinusoidal and biparabolic wave forms, we give numerical values for the energy influx. This result must be contrasted with a previous article, where we have considered the case of moderately high frequencies, when a global hydrodynamic description can be applied [10]. In that case, the expression for the energy influx was different, as well as was the way the limit of high frequencies must be taken.

II. KINETIC THEORY DESCRIPTION

Let us consider a granular system fluidized by a wall that oscillates vertically with a frequency ω and maximum amplitude A. We consider the general case of any wave form as represented in Fig. 1. The grains that collide with it, are reflected elastically, emerging with a normal velocity $c' = 2V_w - c$, where c is the precollisional normal velocity and V_w is the instantaneous velocity of the wall. The tangential velocity is preserved in the collision. The results presented in this article are valid for all dimensions, but the relevant dynamics only take place in the direction perpendicular to the wall.

In the limit of high oscillation frequencies (higher than the mean collision frequency between grains), no hydrody-

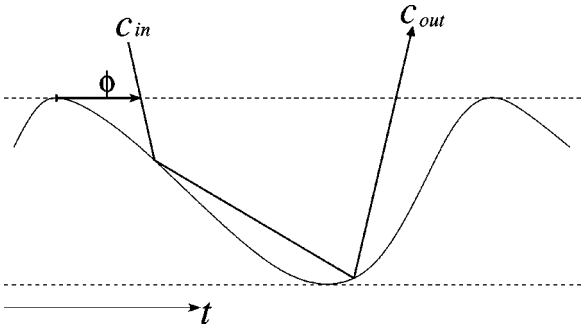

FIG. 1. The generic wave form of the oscillating wall with period $\tau = 2\pi/\omega$ and maximum amplitude A. There is an interaction region (bounded by the two dashed lines). A free particle that collides with the wall enters into the interaction region at a phase ϕ with velocity c_{in} and, after a number of collisions, the particle emerges with a velocity c_{out}.

*Electronic address: rsoto@dfi.uchile.cl

namic theory can be used close to the wall. Indeed, there is a Knudsen layer where only a kinetic approach can be used. We will assume that a Boltzmann-Enskog equation can be used to describe the motion of the system close to the wall. We write the equation for the distribution function $f(\vec{r},\vec{c},t)$ in the compact form

$$\frac{\partial f}{\partial t}+\vec{c}\cdot\frac{\partial f}{\partial \vec{r}}+\vec{g}\cdot\frac{\partial f}{\partial \vec{c}}=J(f,f), \tag{1}$$

where $\vec{g}$ is the external force per unit mass (typically gravity) and J is the collision term. A detailed boundary condition must be supplied to describe the interaction with the oscillating wall.

The system motion is described by two time and length scales. There is the fast and small scale, where the motion is determined by the wall oscillation, and there is a long and slow scale, that describes the macroscopic motion. We change variables to describe the fast scale in full detail:

$$t'=\omega t,\ \ z'=A^{-1}z,\ \ c'=(A\omega)^{-1}c. \tag{2}$$

Rewriting the Enskog-Boltzmann equation in these new variables, we obtain

$$\frac{\partial}{\partial t}f+\vec{c}\cdot\frac{\partial}{\partial \vec{r}}f+(A\omega)^{-1}\omega^{-1}\vec{g}\cdot\frac{\partial}{\partial \vec{c}}f=(A\omega)\omega^{-1}J(f,f), \tag{3}$$

where we have suppressed the primes.

Equation (3) can be highly simplified at high frequencies. If $g/A\omega^2\ll 1$, the term proportional to the gravity acceleration becomes negligible. Analogously, the right-hand side is proportional to the mean collision frequency ν; then if $\nu/\omega\ll 1$, this term can also be neglected. Therefore, in the high-frequency limit, provided the two previous conditions are fulfilled, we can take the first order in ω^{-1} of the above equation

$$\frac{\partial}{\partial t}f+\vec{c}\cdot\frac{\partial}{\partial \vec{r}}f=0. \tag{4}$$

The last equation represents the motion of a free gas, with no collisions and without an external force. That is, in the time and length scale of the wall oscillations, grains do not collide and they do not feel the external force. This result has been obtained independently of the density of the fluid as long as the vibration frequency is much larger than the collision frequency. A pathological situation can be obtained if the system is close to packing near the boundary, because in this case, the collision frequency diverges, making it impossible to take the limit. However, if this were the case, a kinetic theory description also becomes meaningless. Note, however, that in order to arrive to Eq. (4), it is not necessary to assume the Boltzmann-Enskog equation. In fact, the Bogoliubov-Born-Green-Kinkwood-Yvon (BBGKY) equation (derived without approximations from Liouville's equation) for the one-particle distribution has a right-hand side that is also proportional to the collision frequency ν (see, for example, Ref. [4]). Therefore, if $\nu/\omega\ll 1$, Liouville's equation also leads to Eq. (4) by the same limiting process.

Therefore, the distribution function near the wall can be determined by means of the study of a free particle in the presence of an oscillating wall. As the external field vanishes in the limiting case, the motion of the free particle is as follows: the particle enters into the interaction region with a velocity $c_{in}<0$, and after a number of collisions with the wall, it emerges with a velocity $c_{out}>0$, and never again collides with the wall (see Fig. 1).

The outgoing velocity c_{out} is determined in terms of the incoming velocity c_{in}, and the phase ϕ at which the particle entered into the interaction region: $c_{out}=R(c_{in},\phi)$. The function R has been determined analytically in the case of sawtooth and triangular wave forms [2], but the general case needs the use of numerical calculations. We recall that R does not depend on gravity or the nature of collisions.

At the macroscopic scale, the fast oscillations are described in an stochastic way, where the phase ϕ is uniformly distributed over the interval $[0,2\pi)$. Then, given an incoming velocity, there is a distribution of outgoing velocities

$$P(c_{out};c_{in})=\frac{1}{2\pi}\int_0^{2\pi}d\phi\ \delta(c_{out}-R(c_{in};\phi)). \tag{5}$$

This probability distribution depends only on the typical velocity of the oscillating wall. That is, it only depends on the product $A\omega$. Then,

$$P(c_{out},c_{in})=\frac{1}{2\pi A\omega}\int_0^{2\pi}d\phi\ \delta\left[\frac{c_{out}}{A\omega}-R\left(\frac{c_{in}}{A\omega},\phi\right)\right]. \tag{6}$$

If the particles that arrive to the wall have a known velocity distribution f_{in}, the outgoing velocity distribution f_{out} is given by

$$f_{out}(c_{out})=\int_{-\infty}^{0}dc\left|\frac{c}{c_{out}}\right|P(c_{out},c)f_{in}(c). \tag{7}$$

To keep a finite distribution function (such that the different averages are finite), the limit of high frequency must be taken such that $A\omega$ remains finite. Note that this is in contrast with the case where hydrodynamic equations can be used up to the wall, where it is required that $A\omega^{5/4}$ remains finite [10].

III. HEAT FLUX

The energy (heat) flux that is injected into the system can be computed as

$$Q=\frac{m}{2}\int_{-\infty}^{0}dc\ c^3f_{in}(c)+\frac{m}{2}\int_0^{\infty}dc\ c^3f_{out}(c). \tag{8}$$

This expression needs the knowledge of the incoming distribution function f_{in}. This is a complex problem that needs to solve the Boltzmann-Enskog equation in the Knudsen layer, with an asymptotic boundary condition far from the wall given by the hydrodynamic fields (see, for example, Ref. [4]). For simplicity, and to obtain quantitative predictions, we will assume that the incoming distribution is Maxwellian with local values of the density and temperature.

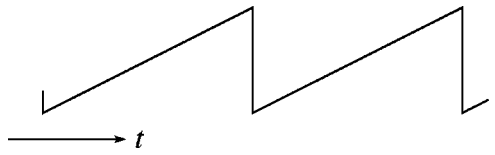

FIG. 2. The motion of the wall in the sawtooth case. The amplitude is A, and the period is $\tau=2\pi/\omega$. The constant upward velocity is $V_0=A\omega/\pi$.

With this assumption, Q can be computed explicitly for a given wave form of the oscillating wall. Equation (8) implies that the heat flux is directly proportional to the local density near the wall. This linear proportionality is not based on the assumption of low density, and it remains valid for dense systems as long as the vibration frequency is much larger than the collision frequency.

We first consider the sawtooth case, where the wall oscillates between $-A$ and A, with a constant upward velocity $V_0=A\omega/\pi$, except for the instant when the wall bounces back to the original position (see Fig. 2). This case has been studied in detail [5–7]. The velocity of the wall when particles collide with it is always V_0. Then, the outgoing velocity of the particle is $c_{out}=2V_0-c_{in}$. Then, $P(c_{out},c_{in})=\delta(c_{out}+c_{in}-2V_0)$.

The heat flux can be computed analytically,

$$Q = m\rho(V_0)^3\left(\frac{T}{mV_0^2}+\sqrt{\frac{2}{\pi}\frac{T}{mV_0^2}}\right), \tag{9}$$

where ρ is the number density near the wall. This result is the same as the one obtained in Refs. [5] and [6] for the dilute case, although here we have shown that this expression is valid for all densities. It is different from the expressions for the energy influx presented in the appendix of Ref. [7] in the cases of small and large temperatures.

The case of a sinusoidal wall $y_w=A\cos(\omega t)$ is more relevant to experiments, but the computations cannot be done analytically. However, the outgoing velocity distribution can be easily computed numerically: particles are sorted out from the incoming Maxwellian distribution and the phase ϕ is chosen from a uniform distribution. Then, collisions are computed systematically until the particle emerges from the interaction region. This procedure ends up with the distribution f_{out} and can be easily implemented in the molecular dynamics (MD) of direct simulation Monte Carlo (DSMC) simulations to mimic the high frequency limit. In Fig. 3, the distribution functions for two different incoming temperatures are presented: $T=0.1m(A\omega)^2$ and $T=2.0m(A\omega)^2$. It is seen that there are nonanalyticities at $c=0$. Also, there is a plateau for positive velocities that is more pronounced for smaller temperatures. It is important to note that the outgoing distributions are very different from a Maxwellian.

The heat flux can be obtained using Eq. (8) with the computed distribution. The result can be expressed as

$$Q = m\rho(A\omega)^3\sqrt{\frac{T}{m(A\omega)^2}}q\left(T/m(A\omega)^2\right), \tag{10}$$

where the function q is presented in Fig. 4. Although it is not uniform it can be well approximated by the constant value

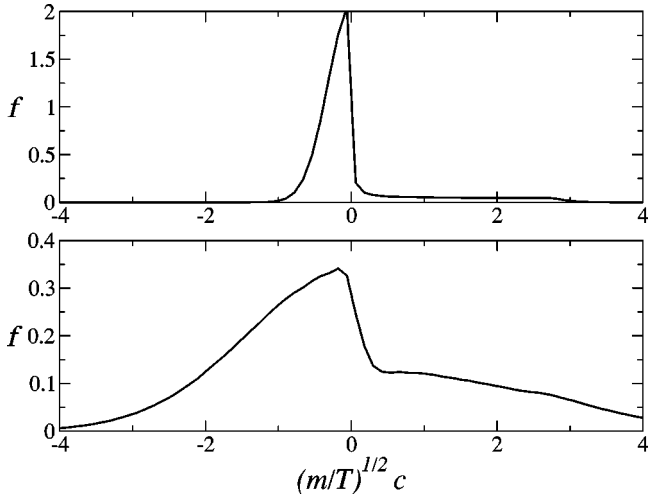

FIG. 3. The velocity distribution by an oscillating wall. The incoming distribution (negative velocities) is a Maxwellian with temperature T. The outgoing distribution is computed using the algorithm described in the text. The top plot corresponds to $T=0.1m(A\omega)^2$ and the bottom plot is for $T=2.0m(A\omega)^2$.

$q\approx 0.8$. This value is in good agreement with the asymptotic prediction for high temperatures $q=\sqrt{2/\pi}\approx 0.798$ [5,8], but the interpolation expression given in Ref. [8] gives only a qualitative agreement (see Fig. 4).

Another oscillating wall that we consider is the one having a biparabolic wave form. It consists in a sequence of parabolas of alternating convexities that mimics the sinusoidal wave form. This wave form is practical in numerical simulations, since particle-wall collisions can be predicted more accurately than in the sinusoidal case. The q function, defined by Eq. (10), can be also computed in this case.

Figure 4 presents the q function for the sawtooth, sinusoidal, and biparabolic cases. It is seen that the sawtooth wave form produces an energy influx that is very different

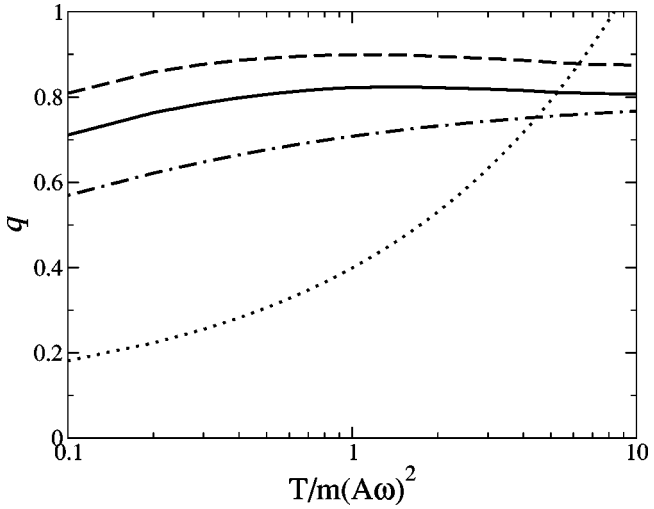

FIG. 4. A comparison of $q[T/m(A\omega)^2]$ for the sinusoidal wave form (continuous line), the biparabolic wave form (dashed line), the sawtooth wave form (dotted line), and the interpolation expression given in Ref. [8] (dashed-dotted line).

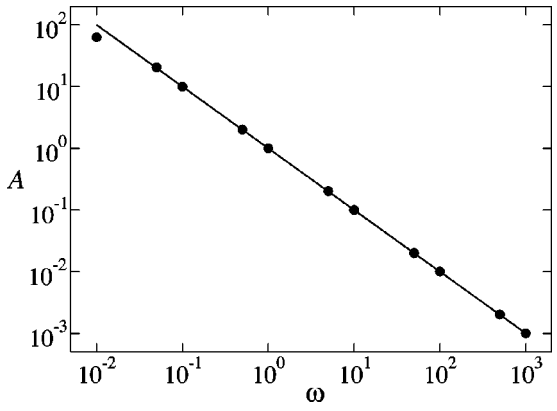

FIG. 5. The optimal value of the amplitude A as a function of the oscillating frequency ω to get the same results as a reference case done with $A=1$ and $\omega=1$. Dots are results from molecular dynamics simulations. The continuous line corresponds to the theoretical prediction $A=\omega^{-1}$.

from the other two cases, both in the numerical values and in the temperature dependence. The biparabolic wave form gives values that approximates qualitatively well the sinusoidal case.

IV. MOLECULAR DYNAMICS SIMULATIONS

To check the validity of our results, we have done MD simulations of a granular system. We have considered the inelastic hard sphere model in two dimensions, where grains are disks of diameter σ and mass m, and the energy dissipated at collisions is modeled with a constant restitution coefficient $\alpha<1$. The system is composed of N grains placed in a rectangular box of size $L_x \times L_y$. There is a gravitational field g pointing downward. The system is periodic in the x direction, the top wall is elastic, while the bottom one oscillates for computational simplicity with a biparabolic wave form, with frequency ω and amplitude A. Units are chosen such that $\sigma=1$ and $m=1$.

The first series of simulations was done with a set parameters such that the system achieves a static stationary state, homogeneous in the x direction and with vertical density and temperature profiles. This series was done with $N=5000$, $L_x=100$, $L_y=500$, $\alpha=0.998$, and $g=0.0002$. A reference simulation was done with $\omega=1.0$ and $A=1.0$, and other simulations were done at different frequencies. For each different frequency, an automatic algorithm looks for the best value of A such that, for the upper half of the simulating box, the temperature profiles were as similar as possible to the reference simulation. The result is a curve $A=A(\omega)$ that is presented in Fig. 5 and, except for $\omega<0.1$, the obtained values agree perfectly with the prediction $A\sim\omega^{-1}$. That the value of the mean collision frequency close to the wall is $\nu=0.21$ explains why the theoretical predictions are valid only for values larger than this one.

Also, in Fig. 6, the temperature profiles are presented for some simulations. It is seen that the macroscopic fields are indistinguishable when the vibration frequency is higher than the collision frequency and when $g/A\omega^2 \ll 1$. This confirms

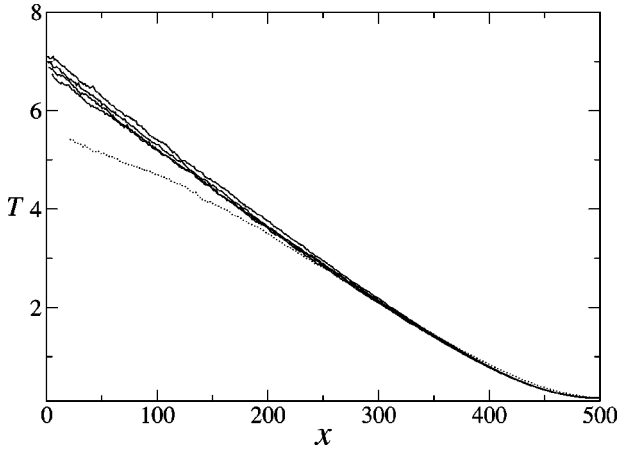

FIG. 6. The temperature profiles obtained in MD simulations for different values of ω and with the best value of A. The continuous lines, form the upper to the lower, correspond to $\omega=1000$ and $A=1.007\times10^{-3}$, $\omega=100$, and $A=1.008\times10^{-2}$, $\omega=1$ and $A=1$, $\omega=0.5$ and $A=2.009$. The dotted line corresponds to $\omega=0.1$ and $A=9.98$.

that the macroscopic fields do not depend on A or ω, but on the product $A\omega$ in the high-vibration frequency limit.

Another simulation was done to check the expression for the heat flux. The parameters of the simulation are chosen such that the system develops a spatial instability [8,11–13] that reaches a steady state with the presence of convective rolls and density modulations.

Figure 7 presents the density field in a simulation done with the following parameters: $\sigma=1$, $m=1$, $N=5000$, $L_x=632.5$, $L_y=79.0$, $g=0.00632$, $\alpha=0.92$, $A=0.01$, and $\omega=100$. The density presents important inhomogeneities in the x and y directions. Besides, there is an important velocity field. Figure 8 presents the density, temperature, and heat flux by the oscillating wall, as a function of x, computed in the MD simulations. All these fields are strongly inhomogeneous and, in particular, it is clearly seen that the temperature at the vibrating wall is not uniform. Therefore, it is incorrect to assume that the vibrating wall imposes a fixed temperature.

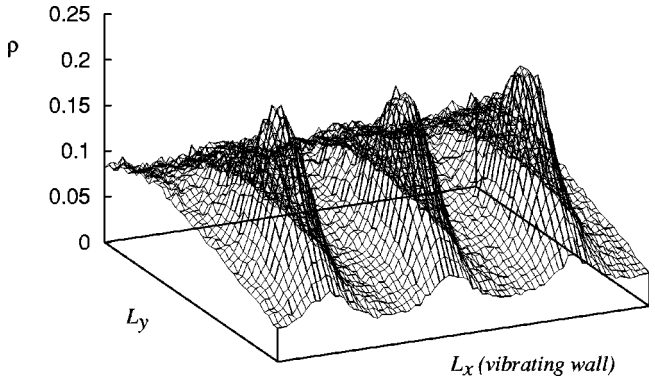

FIG. 7. The density field in the final stationary state of a simulation where the parameters are chosen such that the system develops a spatial instability. There is a vibrating wall and a gravitational field pointing toward the vibrating wall.

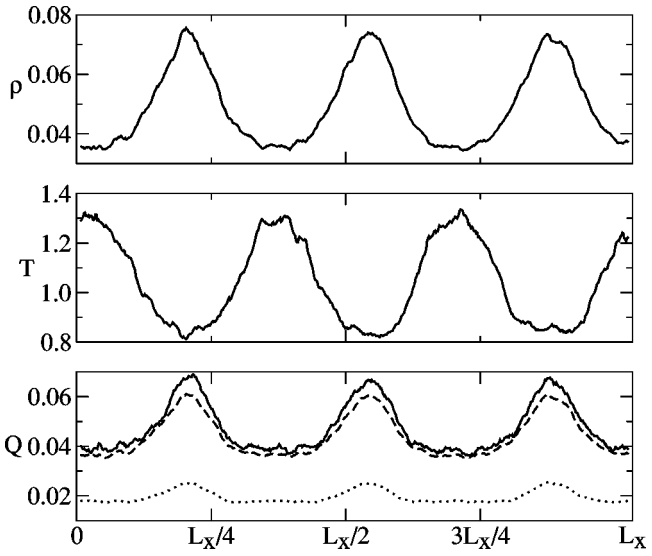

FIG. 8. Density (top), temperature (middle), and heat flux (bottom) profiles by the wall in the stationary regime. The solid lines are the computed values in the MD simulations, and the dashed (dotted) line is the heat flux computed with the theoretical expression for a biparabolic (sawtooth) wave form [Eq. (10) or (9)], using the density and temperature obtained in the simulations.

Also, it presents the computed valued of the heat flux using Eq. (10) with the q function for a biparabolic wave form, taking the local values of density and temperature from the simulations. The comparison between the heat flux obtained in the simulation and the predicted value is excellent. There is a systematic disagreement (the predicted value is slightly smaller that the MD value), probably due to the fact that the incoming distribution is not exactly Maxwellian. The heat flux computed using the q function for the sawtooth wave form disagrees completely with the values from the simulation.

V. CONCLUSION

We have studied a granular system when it is fluidized by a vibrating wall. If the vibration frequency is larger than the grain collision frequency and the wall acceleration is much greater than gravity, a finite limiting case is obtained if the amplitude scales as $A \sim \omega^{-1}$. If two experiments were performed with different oscillation frequencies and amplitudes such that the value of $A\omega$ is preserved, they would produce the same macroscopic flows.

Also, in this limiting case, it is shown that for the purpose of calculations, the time-dependent kinetic boundary condition can be replaced by a stochastic stationary boundary. If the incoming velocity distribution is close to a Maxwellian, this stationary boundary injects heat, where the value of the injected heat is proportional to the local density at the wall and it depends on the local temperature at the wall, and on the wave form of the oscillating wall. The strict linear dependence with density is valid even for dense cases, where nonideal effects can be present. Also the value of the energy influx is independent on any external field or on the restitution coefficient between particles. Explicit analytic and numerical expressions were found for the sawtooth and sinusoidal walls, respectively. The heat flux produced by the sinusoidal and the sawtooth wave form are very different, and the latter cannot be used as a model to estimate the energy influx in a sinusoidal vibrating wall. However, the biparabolic wave form correctly describes (with an error of 12%) the heat flux produced by the sinusoidal wave form. The comparison of the predictions with MD simulations is excellent in verifying the scaling and the expression for the heat flux. In the simulation it is verified that replacing the vibrating wall by a thermal wall is a poor approximation, especially when there are spatial inhomogeneities, while the replacement by a heat flux source gives excellent results.

ACKNOWLEDGMENTS

The author is grateful for the support of FONDAP through Grant No. 11980002, and the FONDECYT through Project No. 1030993. The simulations were done in the CIMAT's parallel cluster.

[1] J. T. Jenkins and S. B. Savage, J. Fluid Mech. **130**, 187 (1983); J. T. Jenkins and M. W. Richman, Arch. Ration. Mech. Anal. **87**, 355 (1985); J. J. Brey, M. J. Ruiz-Montero, and D. Cubero, Phys. Rev. E **54**, 3664 (1996); C.Bizon, M. D. Shattuck, J. B. Swift, and H. L. Swinney, *ibid.* **60**, 4340 (1999).

[2] S. Warr and J. M. Huntley, Phys. Rev. E **52**, 5596 (1995).

[3] S. McNamara and J.-L. Barrat, Phys. Rev. E **55**, 7767 (1997); S. McNamara and S. Luding, *ibid.* **58**, 813 (1998).

[4] H. Ferziger and H. G. Kaper, *Mathematical Theory of Transport Process in Gases* (North-Holland, Amsterdam, 1972).

[5] V. Kumaran, Phys. Rev. E **57**, 5660 (1998).

[6] J. J. Brey, M. J. Ruiz-Montero, and F. Moreno, Phys. Rev. E **62**, 5339 (2000).

[7] S. R. Dahl *et al.*, Phys. Rev. E **66**, 041301 (2002).

[8] E. Livne, B. Meerson, and P. V. Sasorov, Phys. Rev. E **65**, 021302 (2002); e-print cond-mat/0008301.

[9] W. A. M. Morgado and E. R. Mucciolo, Physica A **311**, 150 (2002).

[10] Rodrigo Soto and M. Malek Mansour, Physica A **327**, 88 (2003).

[11] R. Ramírez, D. Risso, and P. Cordero, Phys. Rev. Lett. **85**, 1230 (2000).

[12] M. Argentina, M. G. Clerc, and R. Soto, Phys. Rev. Lett. **89**, 044301 (2002).

[13] J. J. Brey, M. J. Ruiz-Montero, F. Moreno, and R. García-Rojo, Phys. Rev. E **65**, 061302 (2002).